Classification of Light Sources Using a Quantum Artificial Neuron

Diego Guerrero

February 8, 2026

Abstract

A quantum perceptron was implemented using amplitude encoding on quantum hypergraph states and trained to classify light sources as coherent or thermal. While the evaluation of the perceptron is performed as a quantum process, the training stage was carried out classically using genetic algorithms. A classification accuracy of 93.37% was achieved in noiseless quantum simulations. In contrast, simulations using fake noisy backends showed a significantly lower accuracy of approximately 50%. This degradation in performance is conjectured to arise from the encoding of the hypergraph states and the large circuit depth required for their implementation.

1 Introduction

There exist two main types of light relevant in quantum optics: coherent light and thermal light. Coherent light is typically associated with controlled light sources such as lasers, while thermal light is commonly linked to environmental or chaotic sources and exhibits stronger correlations. Distinguishing between these two types of light is crucial for several technological and experimental applications.

2 The Quantum Perceptron

The quantum perceptron computes the projection between two quantum states in which information is encoded in the amplitudes of the computational basis. Let $|\psi_i\rangle$ be the input state and $|\psi_w\rangle$ the weight state. The perceptron output corresponds to the squared overlap between these two states.

To implement this, two unitary transformations U_i and U_w are defined. The unitary U_i maps the reference state $|0\rangle^{\otimes m}$ to the input state $|\psi_i\rangle$, while U_w maps the weight state to the computational basis state $|1\rangle^{\otimes m}$. The action of these unitaries can be interpreted as rotations in Hilbert space: U_i rotates the reference vector into the input state, and U_w rotates the weight state onto the vertical axis.

Since the overlap is invariant under unitary transformations, it is sufficient to prepare $|\psi_i\rangle$ and then apply U_w. The resulting projection is equivalent to the projection of the transformed input state onto $|1\rangle^{\otimes m}$. This quantity can be extracted using an ancilla qubit entangled with all system qubits through a multi-controlled NOT gate, as shown in Fig. 1.

The classical input and weight vectors are defined as

$$\vec{i} = \begin{bmatrix} i_0 \\ i_1 \\ \vdots \\ i_{m-1} \end{bmatrix}, \quad \vec{w} = \begin{bmatrix} w_0 \\ w_1 \\ \vdots \\ w_{m-1} \end{bmatrix}, \quad i_j, w_j \in \{-1, 1\}. \tag{1}$$

The corresponding quantum states are

$$|\psi_i\rangle = \frac{1}{\sqrt{m}} \sum_{j=0}^{m-1} i_j \, |j\rangle \,, \tag{2}$$

$$|\psi_w\rangle = \frac{1}{\sqrt{m}} \sum_{j=0}^{m-1} w_j \, |j\rangle \,. \tag{3}$$

The unitaries are defined such that

$$U_i \, |0\rangle^{\otimes m} = |\psi_i\rangle \,, \tag{4}$$

$$U_w \, |\psi_w\rangle = |1\rangle^{\otimes m} \,. \tag{5}$$

A graphical representation of these transformations is shown in Fig. 2.

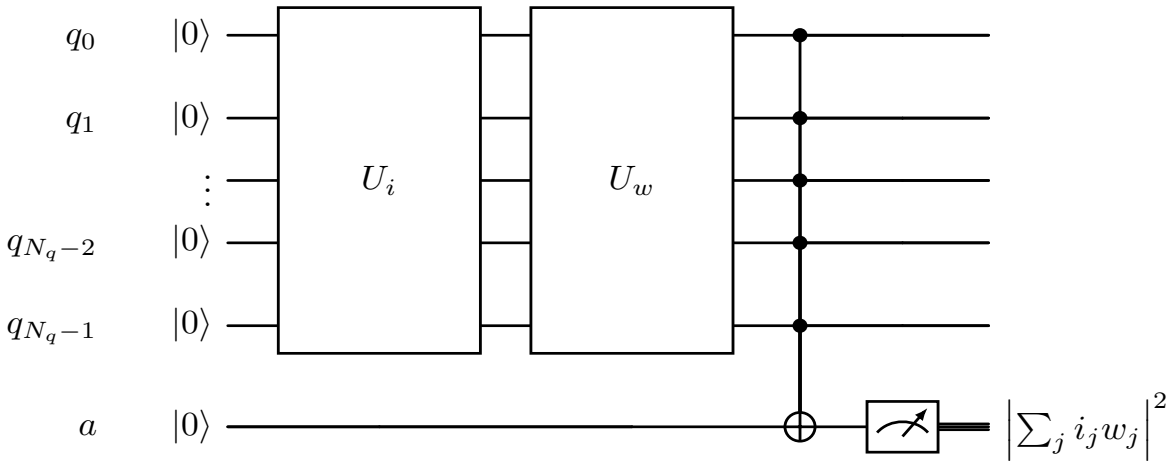

Figure 1: Quantum circuit implementing the quantum perceptron. The ancilla qubit encodes the squared overlap between the input and weight states.

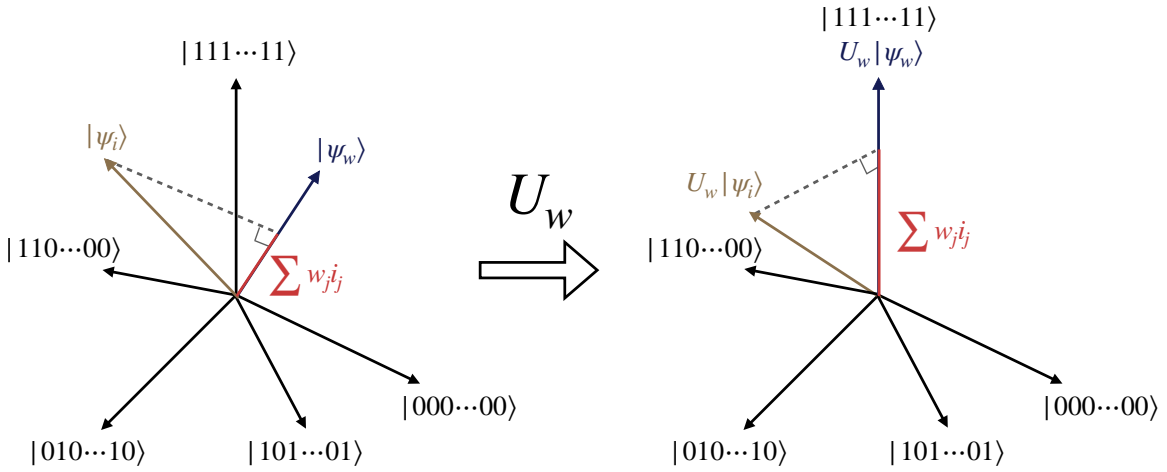

Figure 2: Schematic representation of the unitary transformations U_i and U_w used to compute the state overlap [1].

The definition of the transformations can be done by first realizing that the encoding quantum states are quantum hypergraph states [2].

A quantum hypergraph state is associated with a hypergraph $g_{\leq n} = (V, E)$ of n vertices, where hyperedges may connect any number $k \in \{1, \ldots, n\}$ of vertices. Each vertex is assigned a qubit initialized in the state $|+\rangle$, yielding the initial state $|+\rangle^{\otimes n}$. For every hyperedge connecting qubits $i_1, \ldots, i_k$, a multi-controlled phase gate $C^k Z_{i_1 \ldots i_k}$ is applied. The resulting quantum hypergraph state is

$$|g_{\leq n}\rangle = \prod_{k=1}^{n} \prod_{\{i_1,\ldots,i_k\} \in E} C^k Z_{i_1 \ldots i_k} |+\rangle^{\otimes n},$$

Here results evident that, in order to generate the quantum hypegraph states, the main difficulty is to find the correct sequence of multi controlled z gates.

3 Data Encoding and Training

The experimental data were first converted into binary form and concatenated into a single binary string. This string was then mapped to values in $\{-1, 1\}$ to enable encoding into hypergraph states. The encoding procedure is illustrated in Fig. 3.

Training was performed using a genetic algorithm. An initial population of weight vectors was evolved through crossover operations and random sign flips. This process converged to an optimal weight vector that maximized the classification accuracy. The training was performed in classical computing, ideal quantum computing simulation and noisy quantum simulation.

The unitary transformations, in this particular case, were generated using diagonal matrices that assign a phase of -1 to selected computational basis states, resulting in diagonal unitaries with entries ± 1, defined as the following:

$$U_i' = \mathrm{diag}(\vec{i}^{\,T}), \tag{6}$$

$$U_w' = \mathrm{diag}(\vec{w}^{\,T}), \tag{7}$$

which leads to

$$U_i = H^{\otimes m} U_i', \tag{8}$$

$$U_w = X H^{\otimes m} U_w'. \tag{9}$$

4 Results

The best performance was obtained when both training and evaluation were carried out using noiseless simulations, as shown in Fig. 4. In contrast, training proved ineffective when the perceptron was executed on real quantum hardware. This discrepancy can be attributed to the extremely large number of gates required to implement the unitary transformations, which can exceed 1.1×10^5 gates after transpilation, as illustrated in Figs. 5 and 6.

5 Discussion

The generation of hypergraph states constitutes the most computationally demanding part of the algorithm and represents the main source of noise. An important open question is whether these states can be generated more efficiently so that the corresponding unitary transformations require fewer gates and yield lower noise levels.

In noisy executions, coherent and thermal light exhibit distinct error patterns. For coherent light, the absolute error oscillates between 0.04 and 0.08, whereas for thermal light it lies in the range 0.14 to 0.20. This suggests that entangled data are more sensitive to noise, possibly due to the stronger correlations present in thermal light.

Finally, it would be desirable to explore whether the optimization process itself can be implemented using quantum protocols. At present, only the inference stage is quantum, while training remains classical. Given the low computational cost of the classical optimization, a fully classical approach may currently be more practical unless a clear quantum advantage can be demonstrated.

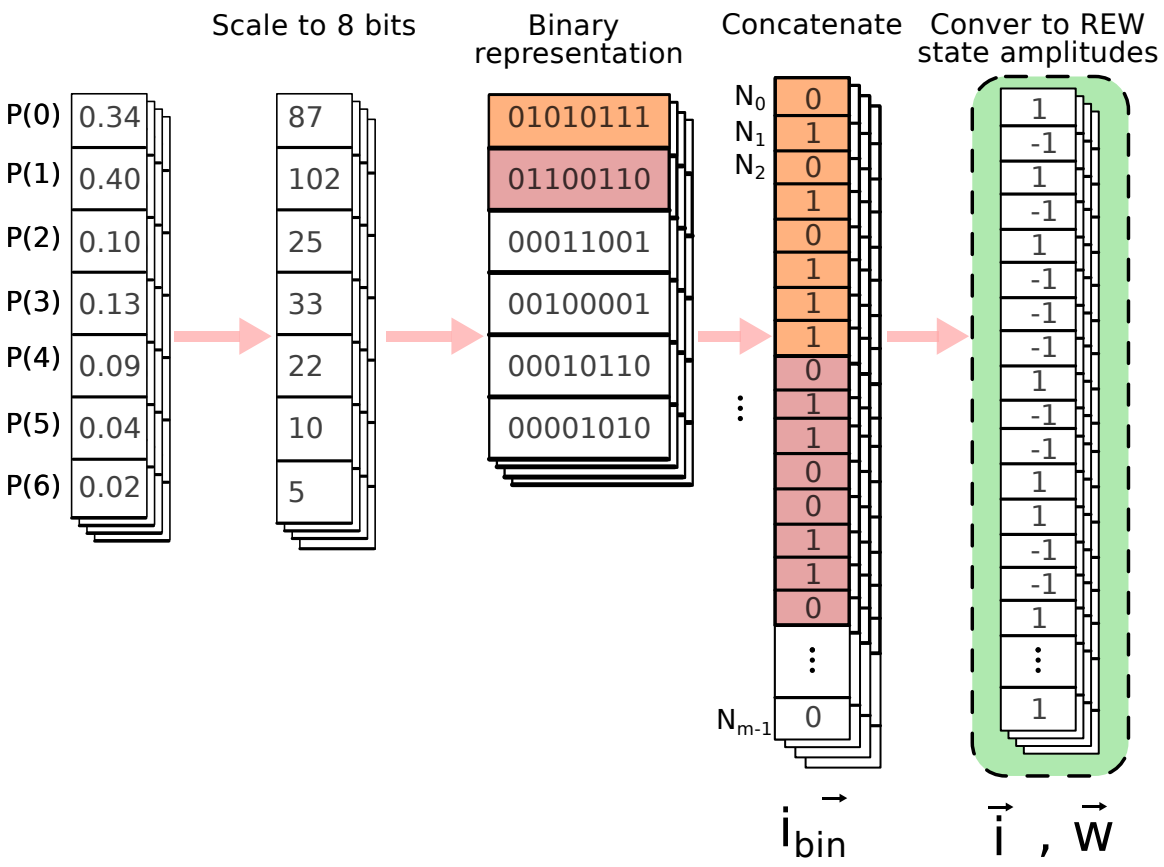

Figure 3: Encoding of classical data into quantum hypergraph states used as input for the quantum perceptron.

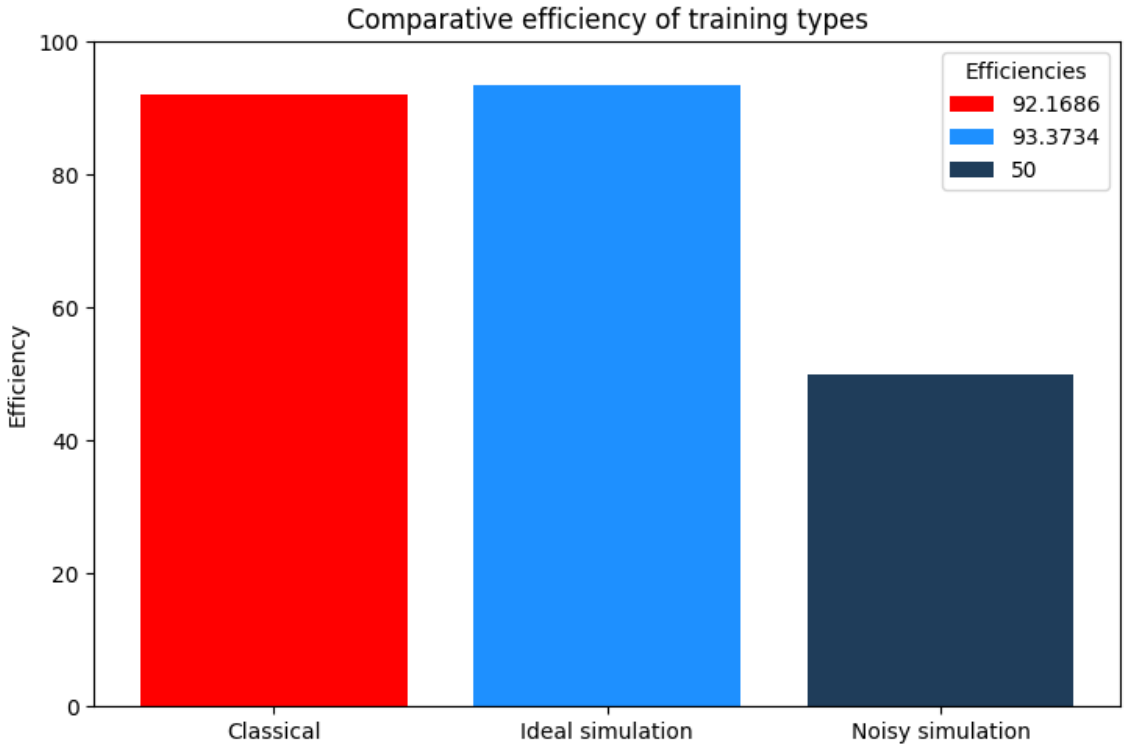

Figure 4: Classification performance on the evaluation set using a training set of 1000 samples.

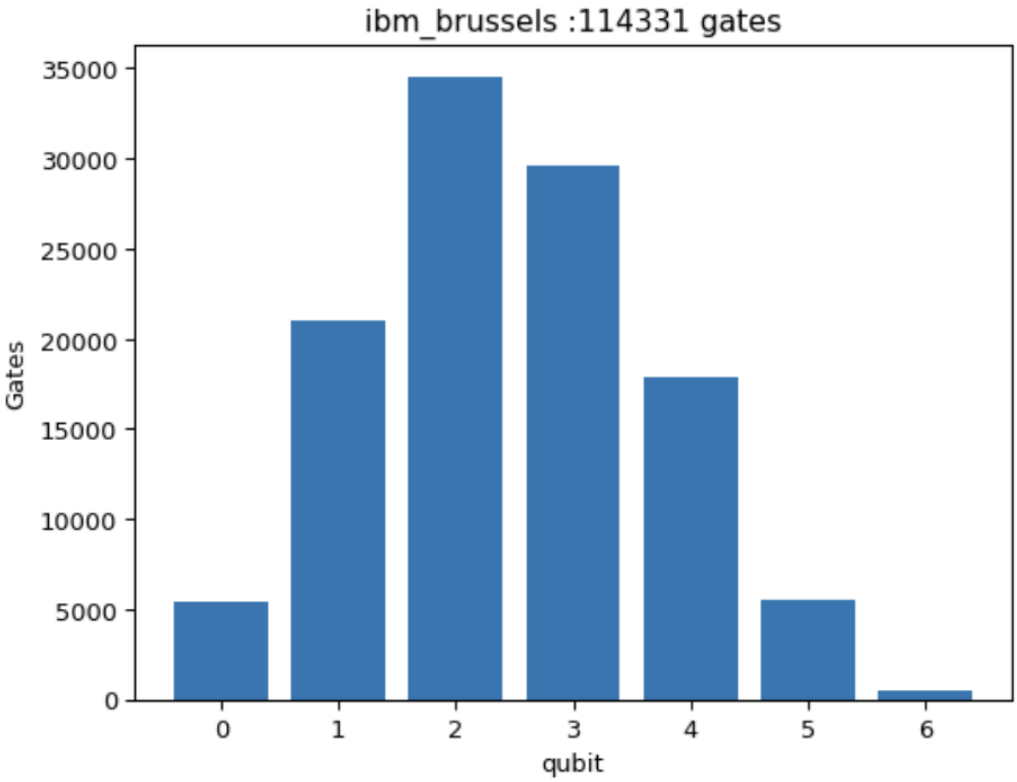

Figure 5: Histogram of the number of gates required to implement the quantum perceptron on the IBM Brussels backend.

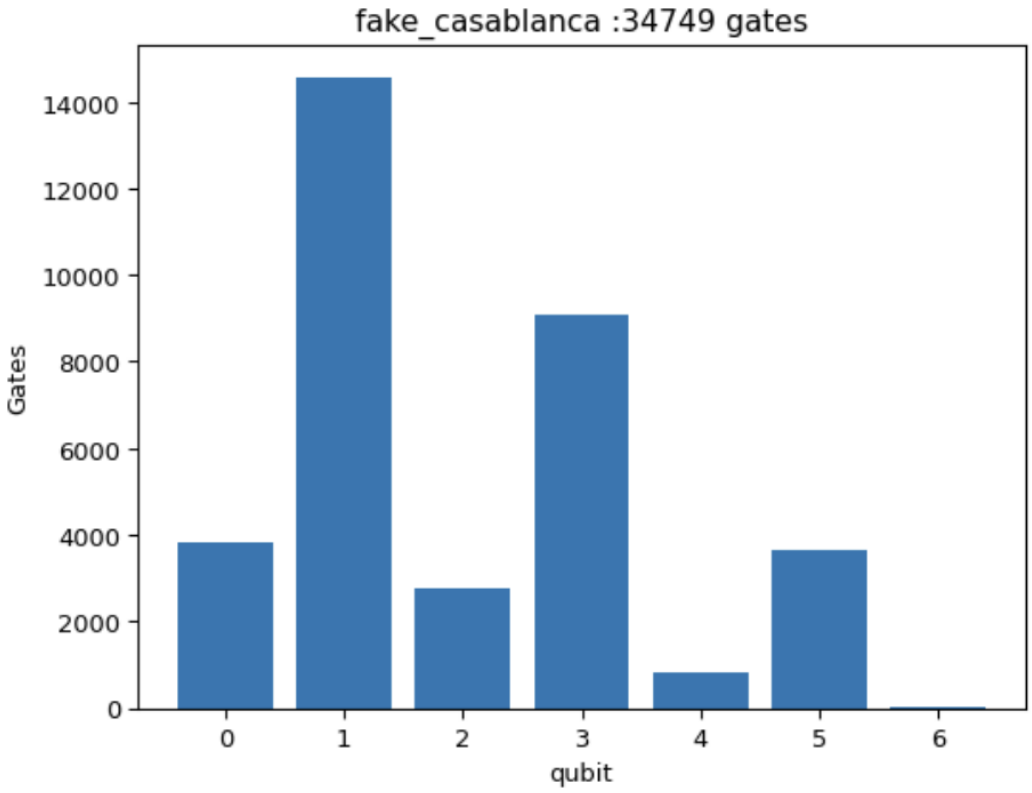

Figure 6: Histogram of the number of gates required for implementation on the 7-qubit IBM Casablanca backend.

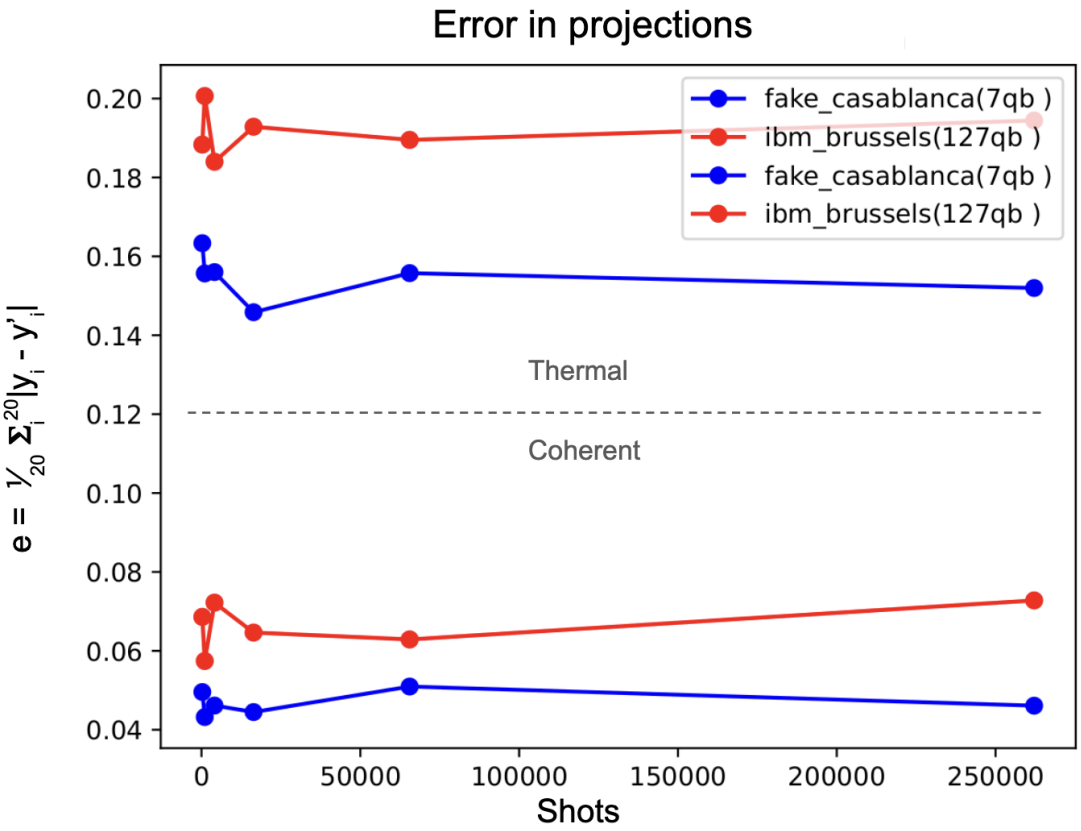

Figure 7: Comparison of the absolute mean error with respect to ideal simulations for fake noisy backends and real quantum processors.

References

[1] Francesco Tacchino et al. "An artificial neuron implemented on an actual quantum processor". In: *npj quantum information* 5.1 (Mar. 2019). DOI: 10.1038/s41534-019-0140-4. URL: https://doi.org/10.1038/s41534-019-0140-4.

[2] M Rossi et al. "Quantum hypergraph states". In: *New Journal of Physics* 15.11 (Nov. 2013), p. 113022. ISSN: 1367-2630. DOI: 10.1088/1367-2630/15/11/113022. URL: http://dx.doi.org/10.1088/1367-2630/15/11/113022.